Journal of Alloys and Compounds 662 (2016) 232–239

Contents lists available at ScienceDirect

Journal of Alloys and Compounds

journal homepage: http://www.elsevier.com/locate/jalcom

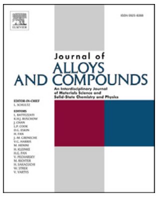

Synthesis and optical performance of a new red-emitting $ZnTiF_6 \cdot 6H_2O:Mn^{4+}$ phosphor for warm white-light-emitting diodes

J.S. Zhong [a], D.Q. Chen [a, b, *], X. Wang [a], L.F. Chen [a], H. Yu [a], Z.G. Ji [a], W.D. Xiang [c]

[a] *College of Materials and Environmental Engineering, Hangzhou Dianzi University, Hangzhou 310018, China*
[b] *State Key Laboratory of Structural Chemistry, Fujian Institute of Research on the Structure of Matter, Chinese Academy of Sciences, Fuzhou 350002, China*
[c] *College of Chemistry and Materials Engineering, Wenzhou University, Wenzhou 325035, China*

ARTICLE INFO

Article history:
Received 8 September 2015
Received in revised form
30 November 2015
Accepted 9 December 2015
Available online 12 December 2015

Keywords:
Photoluminescence
Red phosphor
White LED
Mn^{4+}

ABSTRACT

Mn^{4+}-activated fluoride compounds, emerging as highly efficient rare-earth-free red-emitting phosphors, have been regarded as excellent color converters for warm white-light-emitting diodes recently. In this paper, using a facile two-step co-precipitation approach, we report the synthesis and structure of a novel $ZnTiF_6 \cdot 6H_2O:Mn^{4+}$ red-emitting phosphor as well as its optical performance in detail. Particularly, the as-prepared yellowish $ZnTiF_6 \cdot 6H_2O:Mn^{4+}$ powders exhibit an intense narrow-band Mn^{4+} $^2E_g \rightarrow {}^4A_{2g}$ red emission with internal quantum efficiency of 26.4% upon the excitation of blue light corresponding to $^4A_{2g} \rightarrow {}^4T_{2g}$ transitions of Mn^{4+}. As a consequence, the warm white-light-emitting diodes with tunable correlated color temperature and color rendering index can be easily realized by combining $ZnTiF_6 \cdot 6H_2O:Mn^{4+}$ red phosphor with commercial $YAG:Ce^{3+}$ yellow phosphor on the blue-InGaN chip.

1. Introduction

Over the past decade, white-light-emitting diodes (WLEDs) have gained extensive attention to scientists and engineers due to their admirable merits of energy-saving, long lifetime, high luminous efficacy and environment friendliness [1–3]. There are several approaches to produce phosphor-conversion LEDs. For UV-LED chips pumping phosphors, both doping a single rare earth ion such as Dy^{3+} and co-doping a sensitizer and activator into appropriate single-phase hosts to produce white light can provide good color rendering. However, problems in the luminescence efficiency and manufacture cost are still exists. There is a tradeoff between the luminescence and the color rendering [4–6]. Currently, blue LED chips pumping phosphors as the most widely adapted approach to obtain WLEDs, suffers from some technical weaknesses in practical application due to lack of red emitting components, which leads to high correlated color temperature (CCT) and low color rendering index (CRI) [7–9]. In order to solve this issue, enormous research efforts have been devoted to developing rare-earth (RE) activated sulfide and nitride red phosphors [10,11]. Unfortunately, most nitride-type phosphors require critical preparation conditions and sulfide-type ones are not stable, which limits their application [12]. Therefore, it is highly desirable to develop new phosphors to meet the practical requirements of WLEDs [13].

As an alternative, the non-rare-earth metal ion Mn^{4+}, as an efficient activator for red phosphor, offers several important advantages due to its spectroscopic properties and economic feasibility [14,15]. Compared to the parity-forbidden f–f transition of RE ions, the 3 d^3 electron configuration of Mn^{4+} is easily affected by differently coordinated environments due to the electrons located in an outer orbit [15,16]. Generally, Mn^{4+}-activated phosphor materials exhibit broad adsorption bands spanning from 380 to 490 nm and sharp red emission between 600 and 780 nm [17]. A typical example of Mn^{4+}-doped oxide phosphor is $Sr_4Al_{14}O_{25}$ [14,18,19]. However, its emission is located in the wavelength region between 650 and 680 nm, which is too far red-shifted for efficient warm WLEDs. Meanwhile, most of the Mn^{4+}-activated oxide phosphors are synthesized at a higher temperature, which requires special equipment and thus causes rather high cost [20]. To circumvent the above-mentioned drawbacks, a series of Mn^{4+}-doped fluorides $A_2BF_6:Mn^{4+}$ (A = K, Na, Ba, Rb, Cs and B=Si, Ti, Ge) have been reported, which have a strong and broad absorption band in blue region and emit red luminescence with a emission peak at ~630 nm [21–38]. For example, Adachi et al. prepared a series of $A_2BF_6:Mn^{4+}$ red phosphors using wet chemical etching by mixing metal wafer in a $HF/AMnO_4$ (A = K, Na) solution [26–28].

---

[*] Corresponding author. College of Materials and Environmental Engineering, Hangzhou Dianzi University, Hangzhou 310018, China.
E-mail address: dqchen@hdu.edu.cn (D.Q. Chen).

http://dx.doi.org/10.1016/j.jallcom.2015.12.075

Pan et al. synthesized $K_2SiF_6:Mn^{4+}$, $K_2TiF_6:Mn^{4+}$, $BaSiF_6:Mn^{4+}$ and $BaTiF_6:Mn^{4+}$ by hydrothermal methods and studied their optical properties [29–33]. However, wet chemical etching of metal wafer has some shortcomings such as expensive cost of raw materials and low yield. In addition, high temperature, high pressure and long reacting time are generally required during the hydrothermal synthesis [24]. More recently, Chen et al. demonstrated a convenient chemical route based on cation exchange strategy to fabricate highly efficient $K_2TiF_6:Mn^{4+}$ red phosphor [34]. Liu et al. reported a series of $A_2BF_6:Mn^{4+}$(A = K, Na, Rb and B= Ge, Si, Ti) with high thermal stability and extremely high emission intensity synthesized by chemical co-precipitation at room temperature [35–38].

Herein, a new $ZnTiF_6\cdot6H_2O:Mn^{4+}$ red phosphor is fabricated through a mild chemical co-precipitation method. The synthetic technique is facile and the amount of HF used in our experiment is much lower than those adopted in the previously reported works. The optimum contents of K_2MnF_6 for preparation of $ZnTiF_6\cdot6H_2O:Mn^{4+}$ reach to 9.5 mol%. By encapsulating the as-obtained $ZnTiF_6\cdot6H_2O:Mn^{4+}$ red phosphor with $YAG:Ce^{3+}$ yellow phosphor on a InGaN chip, a high-performance warm WLED with low CCT (3987 K) and high CRI (83.1) is achieved.

2. Experimental and characterization method

2.1. Raw materials

ZnF_2 (AR, 99.0%), TiO_2 (AR, 99.8%), KHF_2 (AR, 99.0%), H_2O_2 (AR, 30 wt.% in H_2O), $KMnO_4$ (AR, 99.5%) and HF (GR, 40%) were purchased from Aladdin Chemistry Co. Ltd. (Shanghai, China) and the commercial YAG: Ce^{3+} was purchased from XinLi Illuminant Co. LTD. All the chemicals were used without further purification.

2.2. Synthesis of $ZnTiF_6\cdot6H_2O:Mn^{4+}$ phosphor

A two-step chemical co-precipitation method was used to synthesize $ZnTiF_6\cdot6H_2O:Mn^{4+}$ red phosphor according to the procedures described in the reports [22,34,36] with some modifications. In our experiments, the $ZnTiF_6\cdot6H_2O$ precursor was formed in the solution and then adding K_2MnF_6 to the solution without the step of drying based on cation exchange, the specific operation route was shown in step 2 of Fig. 1. The reaction process was simpler than that reported by Chen et al. [34], and the consumption of HF solution was about 3 times lower than that reported by Liu et al. [36]. The processes were similar to the cases of $K_2GeF_6:Mn^{4+}$ reported in the literature [35], however, extra KF/HF solution was required to drop into GeO_2/KF/HF solution. The prepared processes of $ZnTiF_6\cdot6H_2O:Mn^{4+}$ were schematically illustrated in Fig. 1. First, pure K_2MnF_6 powder was synthesized as following: 0.5 g $KMnO_4$ and 5 g KHF_2 were completely dissolved in 10 mL HF aqueous solution. After stirring for 30 min, H_2O_2 solution was added drop by drop until the solution turned to yellow. The yellow K_2MnF_6 powder was obtained by filtering, washing with acetone and drying at 70 °C for 2 h. The prepared K_2MnF_6 was identified by X-ray powder diffraction (XRD) using Bruker D8 advance diffractometer operated at 40 kV and 40 mA with Cu Kα radiation at 1.5406 Å, as shown in Fig. 1(a). This procedure can be described by the following reaction [22,36].

$$2KMnO_4 + 2KHF_2 + 8HF + H_2O_2 \rightarrow 2K_2MnF_6 + 6H_2O + 2O_2\uparrow \quad (1)$$

Then, 1.28 g ZnF_2 and 1 g TiO_2 were dissolved in 10 mL HF solution under continuously stirring to form saturated solution, and the solution transformed to milky due to the formation of $ZnTiF_6\cdot6H_2O$. After adding a certain amount of K_2MnF_6 powder in the above solution and stirring for 20 min, yellow powders were precipitated at the bottom of the container. Accordingly, the yellow precipitates were obtained by washing them several times with ethanol and drying at 70 °C for 2 h. The crystallinity of the phosphor was examined by XRD, as shown in Fig. 1(b). Based on the above results, we can conclude that the $ZnTiF_6\cdot6H_2O$ first formed in the solution, and then the Ti^{4+} ions in $ZnTiF_6\cdot6H_2O$ crystal were replaced by the Mn^{4+} ones after the introduction of K_2MnF_6 into the solution. The overall reaction responsible for formation of $ZnTiF_6\cdot6H_2O:Mn^{4+}$ can be given as follows:

$$ZnF_2 + (1\text{-}x)TiO_2 + 4(1\text{-}x)HF + (4\text{-}2x)H_2O + xK_2MnF_6 \rightarrow Zn(Ti_{1\text{-}x}Mn_x)F_6\cdot6H_2O + 2xKF \quad (2)$$

For comparison, the $ZnTiF_6\cdot6H_2O$ white powder was also obtained under the same process as step 2 without adding K_2MnF_6, and its crystal structure is shown in Fig. S1.

2.3. LED fabrication

The WLEDs were fabricated by combining the commercial 5 wt% $YAG:Ce^{3+}$ yellow phosphor, $ZnTi_{1\text{-}x}F_6\cdot6H_2O:xMn^{4+}$ (x = 9.5 mol%) red phosphor and blue InGaN chip (457 nm). The phosphors were mixed with silicone resin (HITACHEM-2931 A and B) completely. And the as-obtained mixture of phosphor and silicone was coated on the surface of InGaN chip.

2.4. Characterization

The purity and structure of the as-obtained phosphors were characterized by XRD at a scanning rate of 0.05°/s ranged from 10° to 80°. The X-ray Rietveld refinement data were collected over a 2θ range from 15° to 120° at intervals of 0.01° and analyzed using the Total Pattern Analysis Solutions software. The surface morphologies and structures of the obtained phosphors were observed using a scanning electron microscope (SEM, FEI, operated at an acceleration voltage of 15 kV) with an attached energy-dispersive X-ray spectrometer (EDS). The thermal stability behavior was investigated by thermogravimetrics (TG) analysis (Netzsch STA 449C). The photoluminescence (PL) properties of the phosphors were measured using a fluorescence spectrometer (Edinburgh Instrument FS5) equipped with a 150 W continuous and pulsed Xenon lamp as excitation sources, and the internal quantum efficiency (QE) was detected using an integrating sphere coated with barium sulfate. The photoelectric properties including luminous efficiency (LE), CCT, CRI and Commission International de I'Eclairage (CIE) chromaticity coordinates of the fabricated WLED devices were evaluated using an integrating sphere (HAAS-2000; Everfine Photo-E-Info Co. Ltd, Hangzhou, China) at an operating current of 20 mA.

3. Results and discussion

XRD patterns of the synthesized $ZnTiF_6\cdot6H_2O$ with different K_2MnF_6 contents are shown in Fig. 2(a), along with its corresponding standard diffraction cards ($ZnTiF_6\cdot6H_2O$ JCPDS card no.87-1595 and K_2MnF_6 JCPDS card no.34-0733). When the doping of K_2MnF_6 concentration is less than 11 mol%, all the diffraction peaks can be indexed to hexagonal $ZnTiF_6\cdot6H_2O$ phase (JCPDS card no.87-1595). No traces of K_2MnF_6 residual and other impurity phases are found, which indicates that the doping of K_2MnF_6 does not change the crystal structure of $ZnTiF_6\cdot6H_2O$. However, when the K_2MnF_6 concentration is more than 12.5 mol%, some diffraction peaks of impurity phase belonging to K_2MnF_6 are observed. As the content of Mn^{4+} reaches as high as 21.5 mol%, the XRD pattern matches well with the standard card of K_2MnF_6 (no.34-0733).